Study on low-order aberration measurements of large-aperture flats based on scanning pentaprism technology

ERHUI QI,* HAIXIANG HU, AND XIAO LUO

Key Laboratory of Optical System Advanced Manufacturing Technology (KLOMT), Changchun Institute of Optics, Fine Mechanics and Physics, Chinese Academy of Sciences, Changchun, 130033 Jilin, China
*Corresponding author: qieh@ciomp.ac.cn

Received 3 July 2018; revised 1 October 2018; accepted 23 November 2018; posted 30 November 2018 (Doc. ID 336087); published 22 January 2019

Pentaprism scanning technology (PPS) is an absolute testing method that has the advantages of a simple structure and absolute testing without an extra reference flat, as well as being able to provide *in situ* surface measurements, and more. It plays an important role in the manufacturing process of large flat mirrors. For calibrating the PPS's uncertainty, this paper describes a multi-mode scanning method to implement the measurement of low-order aberrations and introduces the concept of an autocorrelation coefficient to evaluate the data processing progress. These improvements were applied to the measurement of a large flat mirror (1630 mm in diameter), which demonstrates that the measuring uncertainty of PPS can be about 20 nm rms. Furthermore, in regard to the special requirements of M3MP, the prototype mirror of M3M (the tertiary mirror) in the Thirty Meter Telescope project with a non-circular aperture, we analyzed the slope distribution of low-order aberrations, power, and astigmatism. The sample route lines of PPS are then reorganized and a new data process algorithm is implemented. This work was performed in order to improve the PPS's performance in measuring low-order aberrations of large flat mirrors. © 2019 Optical Society of America

https://doi.org/10.1364/AO.58.000787

1. INTRODUCTION

Large flat mirrors play an important role in optical systems; they are usually used as reflection mirrors in big telescope systems, transmission lenses of large interferometers, and standard mirrors in some optical systems. With development of telescopic technology [1–4], a larger dimension of flat mirror is needed and higher accuracy of the surface measurement is required. For example, the Thirty Meter Telescope's (TMT's) [5,6] tertiary mirror (M3M) is 3.5 m × 2.5 m, which is the largest flat mirror in development. How to solve the problem of measuring ultra-large flats like M3M is a big challenge for optical engineers.

Traditional methods like the Ritchey–Common [7] and Fizeau interferometer tests are not practical for testing a large-aperture flat mirror like M3M. The Ritchey–Common test needs a standard sphere with the same size grade, and the testing system is hard to construct. Limited by the size of the reference flat, interferometer testing requires many apertures for stitching, and sub-aperture stitching [8–10] cannot obtain the testing accuracy of low-order aberrations, especially power and astigmatism.

Pentaprisms have the unique advantage of deflecting light beams at a constant angle (nominally by 90°) regardless of their orientation in the line of sight direction. Using this advantage, surface profiles of large flat mirrors can be achieved by measuring slope variations. Pentaprism scanning technology (PPS) is an absolute testing method that uses the mirror itself as the reference, and high-quality references are not needed.

PPS was not first used in optical testing; it has been used to make ultraprecise surface topographic measurements [11,12]. At the Key Laboratory of Optical System Advanced Manufacturing Technology (KLOMT), Changchun Institute of Optics, Fine Mechanics and Physics (CIOMP), we are working on several large flat mirrors for the TMT-M3M project. One mirror has a 1.5 m circular aperture and will be used as the Transmission Flat (TF1500) for testing the slope-RMS of M3M. Another is a 1.63 m circular flat (RF1630) that will be used for calibrating the TF1500 and has a high requirement of low-order aberrations, especially power and astigmatism. The third mirror, the M3MP [13], is the prototype of TMT-M3M. It has an elliptical aperture of 900 mm × 600 mm and has the same requirements as the real M3M. This paper introduces a multi-mode method to calibrate PPS's measuring uncertainty and applies this method to the measurement of RF1630. As for the elliptical mirror M3M, this paper demonstrates a new data processing progress and

new scanning path, related works that are applied to the fabrication of M3MP.

2. BASIC PRINCIPLE

As shown in Fig. 1, a pentaprism can deviate the incident beam perfectly 90 deg to the test surface regardless of the orientation in the pitch direction. Thus, the result measurements are independent of prism alignment, and for this reason, the pentaprism can be used to scan the testing surface [11].

The principle [14] of a PPS is shown in Fig. 2, where two pentaprisms (one is reference prism A, the other, scanning prism B) are co-aligned to a high-accuracy autocollimator (autocollimator1 in Fig. 2). The measuring beam comes out from the autocollimator, deviated by the pentaprism to the mirror surface, then the reflected beam takes the surface information back. The autocollimator can measure one single signal one time, so two electronic-controlled shutters are designed for alternatively selecting the reference and the scanning signal. The difference between the reference and the scanning signals represent the surface slope varieties, as shown in Eq. (1) as follows:

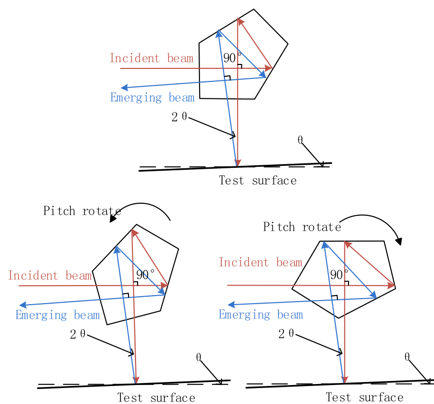

Fig. 1. Principle of a pentaprism.

$$\theta = \frac{1}{2}(V_{\text{scan}} - V_{\text{ref}}), \tag{1}$$

in which V_{scan} represents the slope information brought back by the measuring beam through the scanning prism, and V_{ref} represents the slope information brought back by the measuring beam through the reference prism. Using this referencing measurement, some common errors for both prisms, such as the rotation of the autocollimator and the tilt of the tested mirror, will be avoided. By performing scanning of different lines, the whole surface's profile can be measured.

While performing scanning of the lines, the angular motion of the scanning pentaprism will introduce additional errors to the measuring point, so another autocollimator (Autocollimator 2 in Fig. 2) is used to construct a feedback control of the angular motions of the scanning pentaprism.

3. APPLICATIONS AND ANALYSIS

A. Multiple-Mode Scanning

In optical manufacturing, Zernike polynomials [15,16] are usually used to express the surface error of optical mirrors. PPS measures the slope data of the surface, and a suitable data processing method is fitting with Zernike slope functions. Table 1 shows several items of Zernike slope functions derived from Zernike polynomials. If the surface error is described by

$$S(x,y) = \sum_{i=1}^{J} x_i \cdot Z_i(x,y), \tag{2}$$

where Z_i are Zernike polynomials in Cartesian coordinates and x_i are their coefficients, and the direction of scanning motion is defined by

$$\vec{i}\cos\theta + \vec{j}\sin\theta, \tag{3}$$

then the surface slope error along the scanning direction can be expressed as

$$g(x,y,\theta) = \sum_{i=1}^{J} x_i \cdot \nabla Z_i(x,y) \cdot (\vec{i}\cos\theta + \vec{j}\sin\theta), \tag{4}$$

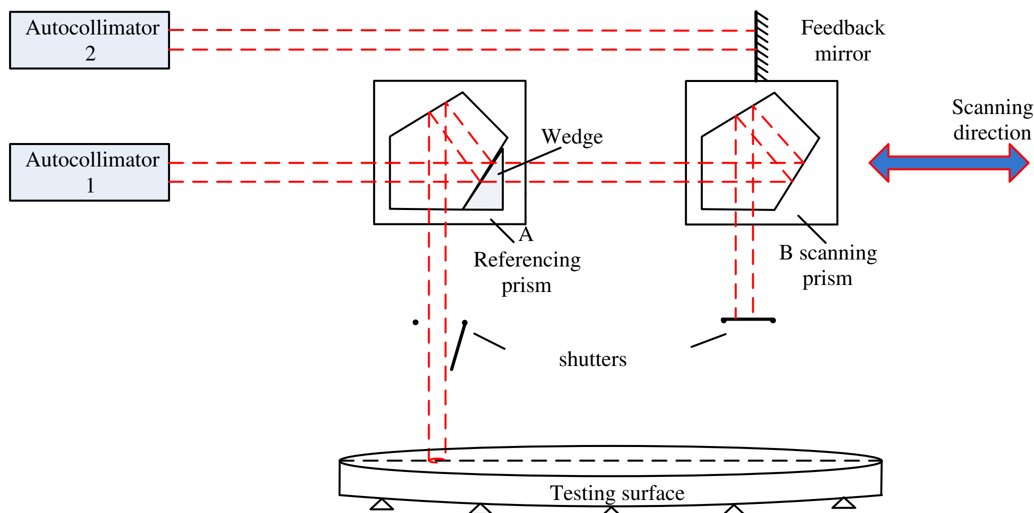

Fig. 2. Principle of the pentaprism scanning system.

Table 1. Zernike Polynomials and Slope Functions

Aberrations	Zernike Polynomials	Gradients
Power	$Z_4 = 2(x^2 + y^2) - 1$	$4x\vec{i} + 4y\vec{j}$
Cos astigmatism	$Z_5 = x^2 - y^2$	$2x\vec{i} - 2y\vec{j}$
Sin astigmatism	$Z_6 = 2xy$	$2y\vec{i} + 2x\vec{j}$
Cos coma	$Z_7 = 3(x^3 + xy^2) - 2x$	$(9x^2 + 3y^2 - 2)\vec{i} + 6xy\vec{j}$
Sin coma	$Z_8 = 3(x^2y + y^3) - 2y$	$6xy\vec{i} + (3x^2 + 9y^2 - 2)\vec{j}$
Spherical	$Z_9 = 1 - 6(x^2 + y^2) + 6(x^2 + y^2)^2$	$12x(2x^2 - 1)\vec{i} + 12y(2y^2 - 1)\vec{j}$

where $\nabla Z_j(x, y)$ is the gradient of the Zernike polynomials, and the dot product with the measured direction is the slope value of the Zernike polynomials in the measured direction.

Since the PPS performs a discrete test, we process the original data by a least-squares calculation. In order to further calculate, we express the equation into a matrix type by

$$A\vec{x} = \vec{b}, \tag{5}$$

where A is a $m \times n$ matrix that represents the gradients of the Zernike polynomials, m is the number of sampling points, and n is the number of Zernike polynomials needed. Each element in A is a vector dot production of Zernike polynomials and the scanning direction unit vector;

$$A = \begin{bmatrix} \nabla Z_4(1) & \nabla Z_5(1) & \cdots & \nabla Z_n(1) \\ \nabla Z_4(2) & \nabla Z_5(2) & \cdots & \nabla Z_n(2) \\ \vdots & \vdots & \cdots & \vdots \\ \nabla Z_4(m) & \nabla Z_5(m) & \cdots & \nabla Z_n(m) \end{bmatrix}. \tag{6}$$

$\vec{b}$ is a vector of measured slope variations across the mirror surface. Then we can perform a least-squares calculation expressed by

$$\vec{x} = (A^T A)^{-1} A^T \vec{b}. \tag{7}$$

$\vec{x}$ is a $n \times 1$ vector that consists of the coefficients of the fitted Zernike polynomials. After the coefficients are determined, the Zernike polynomials are used to reconstruct the surface topology of the flat mirror.

When performing data processing, we introduce the concept of correlation coefficient R, which represents the accuracy of the whole calculation process. The definition of R is

$$\vec{e} = \vec{b} - A \cdot \vec{x},$$

$$R = 1 - \frac{\mathrm{var}(\vec{e})}{\mathrm{var}(\vec{b})}. \tag{8}$$

$\vec{e}$ means the residual error of the fitting calculation, and R represents the accuracy of the whole calculation process. If the fitting process is perfectly right, then $\vec{e}$ should be zero and the correlation coefficient R would be 1. The closer the value of R to 1, the smaller the fitting residual error. By checking the R value, we can evaluate the data processing progress and make the measurement result more believable.

Although no extra reference is used, many random factors [12], such as autocollimator uncertainty, angular motions, and thermal effect, etc., still influence the system performance. To get the real surface under test, multiple-mode scanning is introduced, which consists of several tests. Each test is well sampled and measures different areas of the surface.

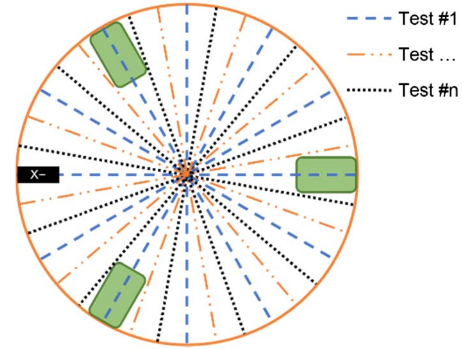

Fig. 3. Schematic of the multi-mode scanning.

As shown in Fig. 3, several tests would be performed. Each test consists of 6 lines' scans, which are separated by 30 deg to make a well-distributed sample of the whole surface. Each test has a base angle, and there is an angle deviation between each two tests. In this way, we can get several independent tests, and each test is well sampled and measures different areas of the surface. PPS uses the flat mirror itself as a reference, no reference error will be introduced, and, after fine alignment of the system [17], there will be no valid systematic error caused by the system hardware. So after all the tests are done, we can take the common part of all the tests as the real surface map, and the deviations between all the tests can be considered as the measuring uncertainty. Unlike methods using the traditional Monte Carlo simulation, the multiple-scanning method is not a simulation result; it can obtain the PPS's final measuring uncertainty intuitively, and a more convincing measurement result can be achieved by this method.

B. Measuring Aberrations That Affect Plate Scale

TMT is one of the several ultra-huge telescopes being constructed; its tertiary mirror (M3M) is a 2.5 m × 3.5 m elliptical flat mirror. M3M has a special requirement related to its low-order aberrations; its power and astigmatism affect the critical calculation of the plate scale [5]. Furthermore, M3M has an elliptical clear aperture, not circular, which limits the use of circular Zernike polynomials. To address this issue, we first shorten the long axis by a factor $\sqrt{2}$, which makes the aperture a circular one, and then the character of plate scale is analyzed.

Plate scale consists of power and astigmatism, which can be expressed by Eq. (2) as

$$Z_4 = 2\rho^2 - 1,$$
$$Z_5 = \rho^2 \cos(2\theta),$$
$$Z_6 = \rho^2 \sin(2\theta). \quad (9)$$

Z_4 represents power, Z_5 is 0 deg astigmatism, and Z_6 is 45 deg astigmatism.

Only considering the low-order aberrations about which M3M cares a great deal, the plate scale can be described by the following Eq. (10), which is a linearity combination of power and astigmatism:

$$Z = a * Z_4 + b * Z_5 + c * Z_6. \quad (10)$$

In Eq. (10), a, b, and c represent the coefficients of Z_4, Z_5, and Z_6, respectively. Changing into polar coordinates, Eq. (10) can be described by

$$Z = a * (2 * \rho^2 - 1) + b * (\rho^2 * \cos(2\theta)) + c * (\rho^2 * \sin(2\theta)). \quad (11)$$

Taking a partial derivation of radius ρ, we can get

$$Z_\rho = 4 * a * \rho + 2 * b * \rho * \cos(2\theta) + 2 * c * \rho * \sin(2\theta). \quad (12)$$

There is only one order radius ρ left except the coefficients; taking the two-order partial derivation of radius ρ, we can then get

$$Z_{\rho\rho} = 4 * a + 2 * b * \cos(2\theta) + 2 * c * \sin(2\theta). \quad (13)$$

After taking the two-order partial derivation of radius ρ, we can see that the plate scale is a function of angle θ. Taking a combination of the trigonometric functions, we can get

$$B = 2\sqrt{b^2 + c^2},$$
$$\phi = \arctan\left(\frac{c}{b}\right),$$
$$Z_{\rho\rho} = 4 * a + 2 * B * \cos(2(\theta - \phi). \quad (14)$$

As shown in Fig. 4, after taking two-order partial derivation of ρ, the plate scale can be described by a cosine function, the coefficient of Z_4 can be represented by the cosine function's global offset, and the coefficients of Z_5 and Z_6 can be represented by the cosine function's amplitude and phase offset.

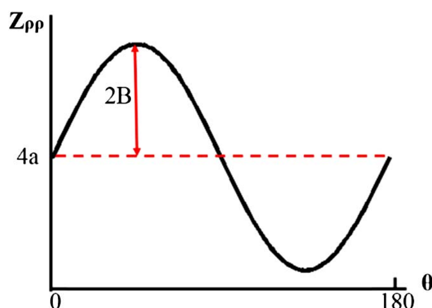

Fig. 4. Form of the plate scale's two-order partial derivation of radius ρ.

Then the measurement changes to characterize a cosine curve. Using this method, we can directly measure power and astigmatism; the original data would be fitted twice, and many random errors would be avoided.

4. OPERATIONS AND EXPERIMENTAL RESULTS

Based on the analysis results in Section 3, PPS was applied to RF1630 and M3MP.

A. Measurement on RF1630

As shown in Fig. 5, the RF1630 mirror was placed on a 4 m rotating table with the PPS hardware bridged placed across it by a 6 m long rail to perform on-site testing. After coarse and fine alignment of the PPS system and the flat mirror, a multi-mode scanning measurement was performed on RF1630.

The RF1630 mirror is supported by three points on the rotate table, as shown in Fig. 6(a). The fine element analysis (FEA) result shows there would be an obvious trefoil on the surface map. As shown in Fig. 6(b), we performed six lines of scanning for each measurement. Each single line is separated by 30 deg, and after one line of scanning is completed, the mirror will rotate 30 deg, and then the next scan will start. As shown in Fig. 6(b), three tests were performed in all. Test #1 scans straight on the middle line of the support blocks,

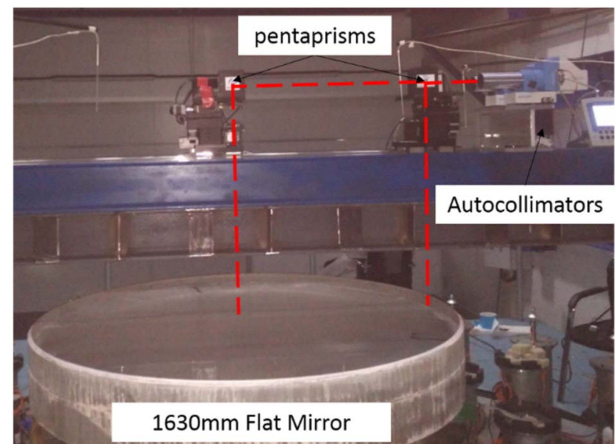

Fig. 5. PPS and the measured flat mirror.

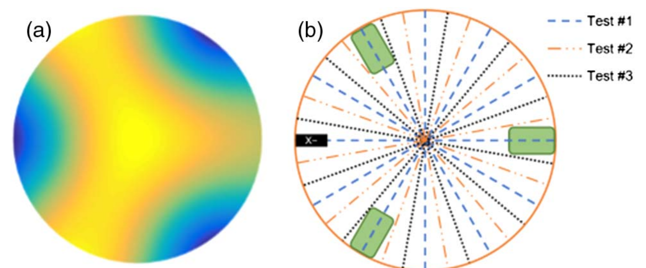

Fig. 6. (a) FEA result of the deformation under three-point support and (b) scanning route settings of the 1.63 m flat; the green blocks represent support.

and test #2 and test #3 have an angle deviation with test #1. If the datum angle of test #1 is defined as 0 deg, then test #2's datum angle will be 10 deg and test #3's datum angle will be 20 deg. The three tests, tests #1–3, formed a multi-mode scanning measurement.

PPS is sensitive to environment, especially temperature and vibrations, so in order to reduce sampling time and reduce environmental impact, only seven points were sampled for each line with 40 seconds of data collection for single point, and then the measuring time for a single complete test can be controlled in less than 1.5 h.

All the measured data was fitted by Zernike slope functions for each measurement, and the fitting accuracy was evaluated. Figure 7 shows the original data and the fitted curves. As shown in Fig. 8, if fitted by Zernike $Z_4 - Z_{16}$, almost all the low-order aberrations, the correlation coefficient R can be bigger than 0.95, approaching the perfect fitting process, which is $R = 1$. If fitted by $Z_4 - Z_6$, as shown in Fig. 9, in which only power and astigmatism are involved, then the correlation coefficient R decreases to about 0.84, which still a convincing fitting progress (in comparison, the confidence level of a Monte Carlo simulation 1σ result is 0.67).

The three tests sampled different areas, the fitting process has great accuracy, and the measured surface has great consistency. So we can take the common part of the three tests as the real surface; as shown in Figs. 8 and 10(a), the measured flat has a PV (the difference between peak and valley value) 2.17λ, rms 0.43λ surface low-order ($Z_4 - Z_{16}$) error, which corresponds to the FEA analysis result shown in Fig. 6(a), and the measured uncertainty of PPS is about 50 nm rms. If considering only power and astigmatism, which we care a great deal about during the fabrication process, the surface error [as shown in Figs. 9 and 10(b)] is 1.57λ in PV and 0.374λ in rms, and the PPS's measured uncertainty can be about 20 nm rms.

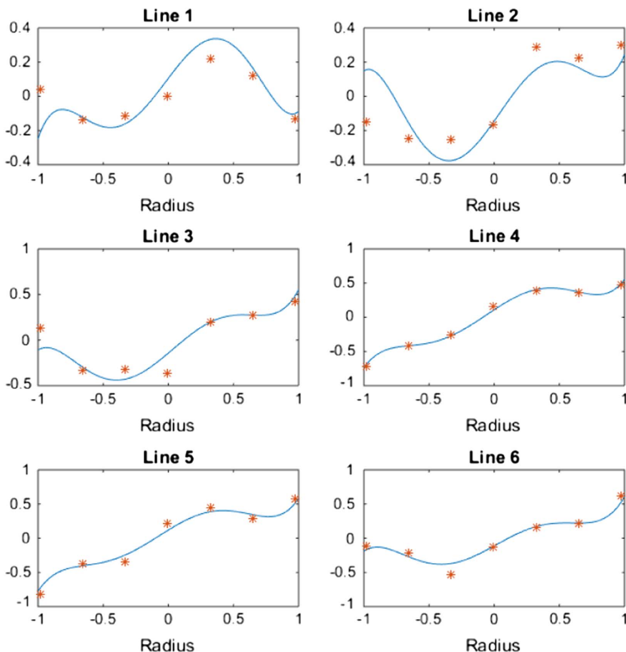

Fig. 7. Original data for each scanning line and the fitted curve in one measurement.

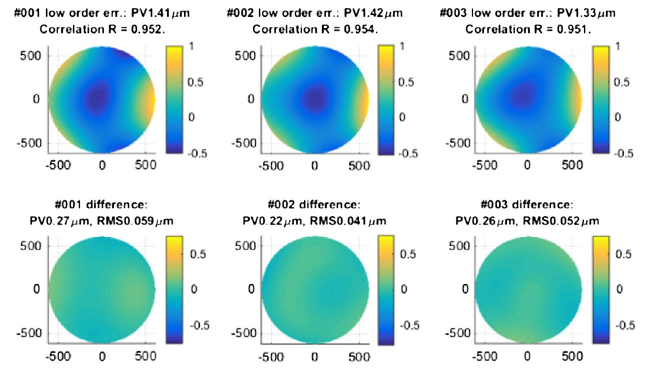

Fig. 8. Measurement results of all the three tests fitted by $Z_4 - Z_{16}$.

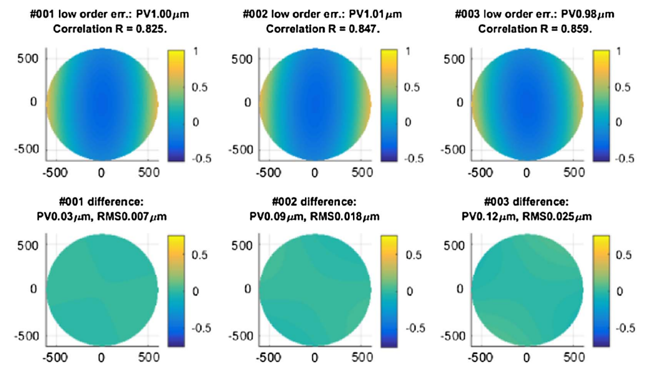

Fig. 9. Measurement results of all the three tests fitted by $Z_4 - Z_6$.

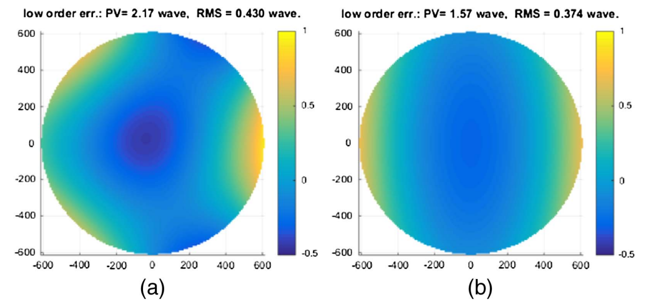

Fig. 10. Measured low-order aberrations. (a) Measured surface map ($Z_4 - Z_{16}$) and (b) measured surface map ($Z_4 - Z_6$).

B. Measurement on M3MP

Before the real M3M mirror, the fabrication of M3MP was first performed in our lab, which has the same requirements as M3M. A special pentaprism scanning system is designed for M3MP; the system is designed to be bridged across the manufacturing rotational table, which provides on-site testing. It is also a kinematic system, which can be lifted and removed when not in use as shown in Fig. 11.

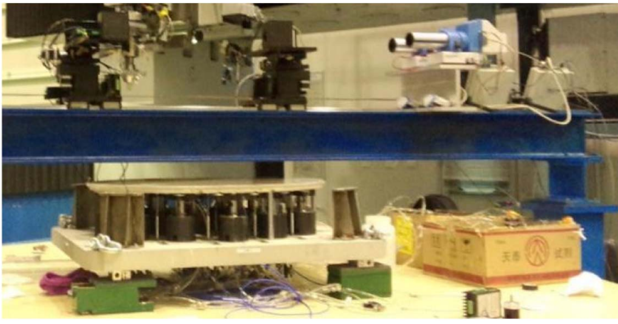

Fig. 11. Measurement on M3MP.

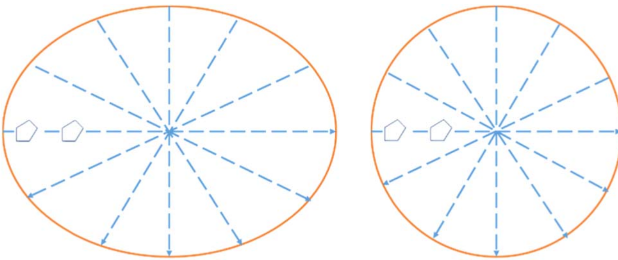

Fig. 12. Scanning routes on elliptical aperture (left) and corresponding circular aperture (right).

After coarse and fine alignment, six lines of scanning were performed to fully describe the cosine function shown by Eq. (14). As shown in Fig. 12, M3MP has an elliptical boundary, so we set the scanning angle of each line as 0, 22.208, 50.768, 90, 129.232, 157.792, and then the corresponding radians in the circular aperture are degree 0, 30, 60, 90, 120, 150, respectively. By performing the six lines of scanning, the data

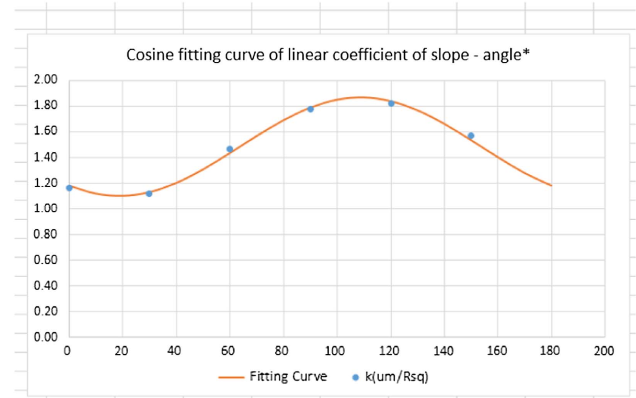

Fig. 14. Cosine fitting curve of the linear coefficient of the slope.

from these lines are fitted to the cosine function shown in Eq. (14), and then the coefficients of the power and astigmatism can be achieved.

After one single line is completed, the table will rotate to the next angle to perform the next line's scanning. Figure 13 shows the original data of each scanning line; to get the full measurement of the whole surface, we set the scanning interval distance as 40 mm, so there will be 13 or 14 measuring points for each scanning line. Some points at the end of the scanning line vary heavily because of the sharp edge of the mirror, which would affect the plate scale calculation greatly, so we take them off when performing data process.

The low-order aberrations from the PPS and the mid- and high-frequency information from the sub-aperture stitching result are combined to guide the polishing progress of M3MP. Figures 13 and 14 show the measured points and the fitted curve for a single test. Figure 15 shows the surface changes before and after one polishing circle, after one polishing recycle; the plate scale, about which M3MP cares a great deal, decreases

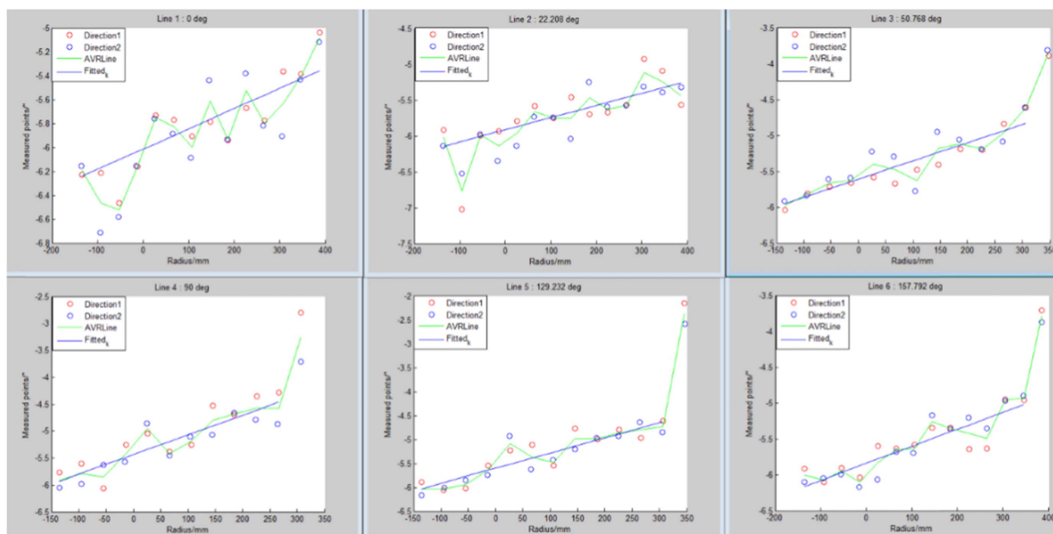

Fig. 13. Original slope data of each scanning line.

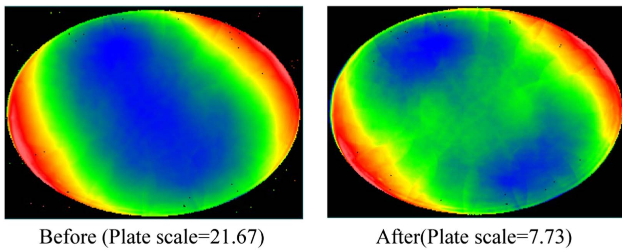

Fig. 15. Surface changes before and after one polishing circle.

from 21.67 to 7.73, and the convergence rate is about 64.3%, proving the practical feasibility of PPS.

5. CONCLUSIONS AND FUTURE WORK

PPS is a reliable absolute test for optical flats. In this paper, we introduced the concept of a correlation coefficient to evaluate the data process progress and developed a multi-mode scanning method to calibrate the PPS's measuring uncertainty. For measuring a non-circular mirror like M3M, we analyzed the character of the plate scale and then designed the scanning route and data processing progress. Guided by PPS, M3MP has a satisfactory single polishing converge rate.

PPS is sensitive to environment, especially temperature and vibrations, so measurements that are an of order of magnitude better can be made with the use of higher-quality hardware (such as rails and pentaprisms) in more controlled environments. We also found that if there are many high-frequency errors on the surface, the fitting residual errors will increase. We will keep on working to improve PPS's performance in measuring large-aperture mirrors.

Funding. National Natural Science Foundation of China (NSFC) (61605202).

REFERENCES

1. W. P. McCray, *Giant Telescopes: Astronomical Ambition and the Promise of Technology* (Harvard University, 2004).
2. J. Reimers, A. Bauer, K. P. Thompson, and J. P. Rolland, "Freeform spectrometer enabling increased compactness," Light Sci. Appl. **6**, e17026 (2017).
3. W. Zhang, H. Zappe, and A. Seifert, "Wafer-scale fabricated thermo-pneumatically tunable microlenses," Light Sci. Appl. **3**, e145 (2014).
4. P. Y. Bely, *The Design and Construction of Large Optical Telescopes* (Springer, 2003).
5. TMT Group, "Tertiary Mirror Surface Fig. Specification," TMT.OPT.SPE.12.001.CCR01.12 (2014).
6. G. H. Sanders, "Managing a big ground-based astronomy project: the Thirty Meter Telescope (TMT) project," Proc. SPIE **7017**, 70170H (2008).
7. S. Han, E. Novak, and M. Schuring, "Application of Ritchey-Common test in large flat measurements," Proc. SPIE **4399**, 131–136 (2001).
8. L. H. Wang, S. B. Wu, and X. Hou, et al., "Flat wavefront measured by subaperture stitching interferometry," Opto-Electron. Eng. **36**, 126–130 (2009).
9. J. G. Thunen and O. Y. Kwon, "Full aperture testing with sub-aperture test optics," Proc. SPIE **0351**, 19–27 (1982).
10. R. Geckeler and I. Weingärtner, "Sub-nm topography measurement by deflectometry: flatness standard and wafer nanotopography," Proc. SPIE **4779**, 1–12 (2002).
11. P. Mallik, C. Zhao, and J. H. Burge, "Measurement of a 2-m flat using a pentaprism scanning system," Proc. SPIE **5869**, 58691A (2005).
12. J. Yellowhair and J. H. Burge, "Analysis of a scanning pentaprism system for measurement of large flat mirrors," Appl. Opt. **46**, 8466–8474 (2007).
13. X. Luo, Q. Erhui, H. Hu, V. G. Ford, and G. Cole, "Fabrication and metrology study for M3MP of TMT," Proc. SPIE **9682**, 968209 (2016).
14. J. E. Yellowhair, "Advanced technologies for fabrication and testing of large flat mirrors," Ph.D. thesis (The University of Arizona College of Optical Sciences, 2007).
15. R. J. Noll, "Zernike polynomials and atmospheric turbulence," J. Opt. Soc. Am. **66**, 207–211 (1976).
16. V. N. Mahajan, "Zernike polynomials and wavefront fitting," in *Optical Shop Testing*, D. Malacara, ed., 3rd ed. (Wiley, 2007), pp. 498–546.
17. R. D. Geckeler, "Optimal use of pentaprisms in highly accurate deflectometric scanning," Meas. Sci. Technol. **18**, 115–125 (2007).

159.226.165.18 {ts '2020-06-22 04:37:55'}